KD5170, a novel mercaptoketone-based histone deacetylase inhibitor that exhibits broad spectrum antitumor activity *in vitro* and *in vivo*

Christian A. Hassig,[1] Kent T. Symons,[1] Xin Guo,[1] Phan-Manh Nguyen,[1] Tami Annable,[1] Paul L. Wash,[1] Joseph E. Payne,[1] David A. Jenkins,[1] Céline Bonnefous,[1] Carol Trotter,[1] Yan Wang,[1] John V. Anzola,[1] Elena L. Milkova,[1] Timothy Z. Hoffman,[1] Sara J. Dozier,[1] Brandon M. Wiley,[1] Alan Saven,[2] James W. Malecha,[1] Robert L. Davis,[1] Jerry Muhammad,[1] Andrew K. Shiau,[1] Stewart A. Noble,[1] Tadimeti S. Rao,[1] Nicholas D. Smith,[1] and Jeffrey H. Hager[1]

[1]Kalypsys, Inc., San Diego, California, and [2]Ida M. and Cecil H. Green Cancer Center, Scripps Green Hospital and Scripps Clinic, La Jolla, California

Abstract

Histone deacetylase (HDAC) inhibitors have garnered significant attention as cancer drugs. These therapeutic agents have recently been clinically validated with the market approval of vorinostat (SAHA, Zolinza) for treatment of cutaneous T-cell lymphoma. Like vorinostat, most of the small-molecule HDAC inhibitors in clinical development are hydroxamic acids, whose inhibitory activity stems from their ability to coordinate the catalytic Zn^{2+} in the active site of HDACs. We sought to identify novel, nonhydroxamate-based HDAC inhibitors with potentially distinct pharmaceutical properties via an ultra-high throughput small molecule biochemical screen against the HDAC activity in a HeLa cell nuclear extract. An α-mercaptoketone series was identified and chemically optimized. The lead compound, KD5170, exhibits HDAC inhibitory activity with an IC_{50} of 0.045 μmol/L in the screening biochemical assay and an EC_{50} of 0.025 μmol/L in HeLa cell–based assays that monitor histone H3 acetylation. KD5170 also exhibits broad spectrum classes I and II HDAC inhibition in assays using purified recombinant human isoforms. KD5170 shows significant antiproliferative activity against a variety of human tumor cell lines, including the NCI-60 panel. Significant tumor growth inhibition was observed after p.o. dosing in human HCT-116 (colorectal cancer), NCI-H460 (non–small cell lung carcinoma), and PC-3 (prostate cancer) s.c. xenografts in nude mice. In addition, a significant increase in antitumor activity and time to endpoint occurred when KD5170 was combined with docetaxel in xenografts of the PC-3 prostate cancer cell line. The biological and pharmaceutical profile of KD5170 supports its continued preclinical and clinical development as a broad spectrum anticancer agent. [Mol Cancer Ther 2008;7(5):1054–65]

Introduction

Classes I and II histone deacetylases (HDAC) form a family of 10 zinc-dependent hydrolases and have emerged as promising new drug targets in cancer therapy (1). Acetylation and deacetylation of histones at lysine residues are generally correlated with transcriptional activation and transcriptional repression, respectively (2). In tumor cells, HDACs are overexpressed or aberrantly recruited to regions of the genome that harbor tumor suppressor genes, resulting in their transcriptional down-regulation or silencing (3). It follows that HDAC inhibition results in the transcriptional activation of tumor suppressor genes, which in turn results in cell cycle arrest or apoptosis (4). More recent work has revealed that HDACs have nonhistone substrates, some of which have been directly implicated in human tumor development, e.g., the canonical tumor suppressor gene p53 (5). Thus, reversible lysine acetylation is a highly regulated process, by which the activity of proteins of diverse function is modulated (6).

Several small molecule synthetic and one natural product HDAC inhibitors have advanced into clinical trials (1, 7). Some of these compounds have shown single-agent safety, pharmacodynamic biomarker induction, and evidence of antitumor activity in a variety of hematologic and solid cancers. Moreover, vorinostat has recently been approved for treatment of cutaneous T-cell lymphoma, thus providing clinical validation of this therapeutic strategy (8). Many of the compounds in clinical development seem to have limitations, including low potency, undesirable safety profiles that include cardiovascular safety issues, and potential for drug-drug interactions via cytochrome P450 inhibition (7). Hence, there remains a significant clinical opportunity for efficacious HDAC inhibitors that are safe and well tolerated.

Received 12/5/07; revised 2/12/08; accepted 2/12/08.

The costs of publication of this article were defrayed in part by the payment of page charges. This article must therefore be hereby marked *advertisement* in accordance with 18 U.S.C. Section 1734 solely to indicate this fact.

Note: Current address for J. Hager: Apoptos: 10835 Road to the Cure, San Diego, CA 92121.

Requests for reprints: Christian A. Hassig, Kalypsys, Inc., 10420 Wateridge Circle, San Diego, CA 92121.

doi:10.1158/1535-7163.MCT-07-2347

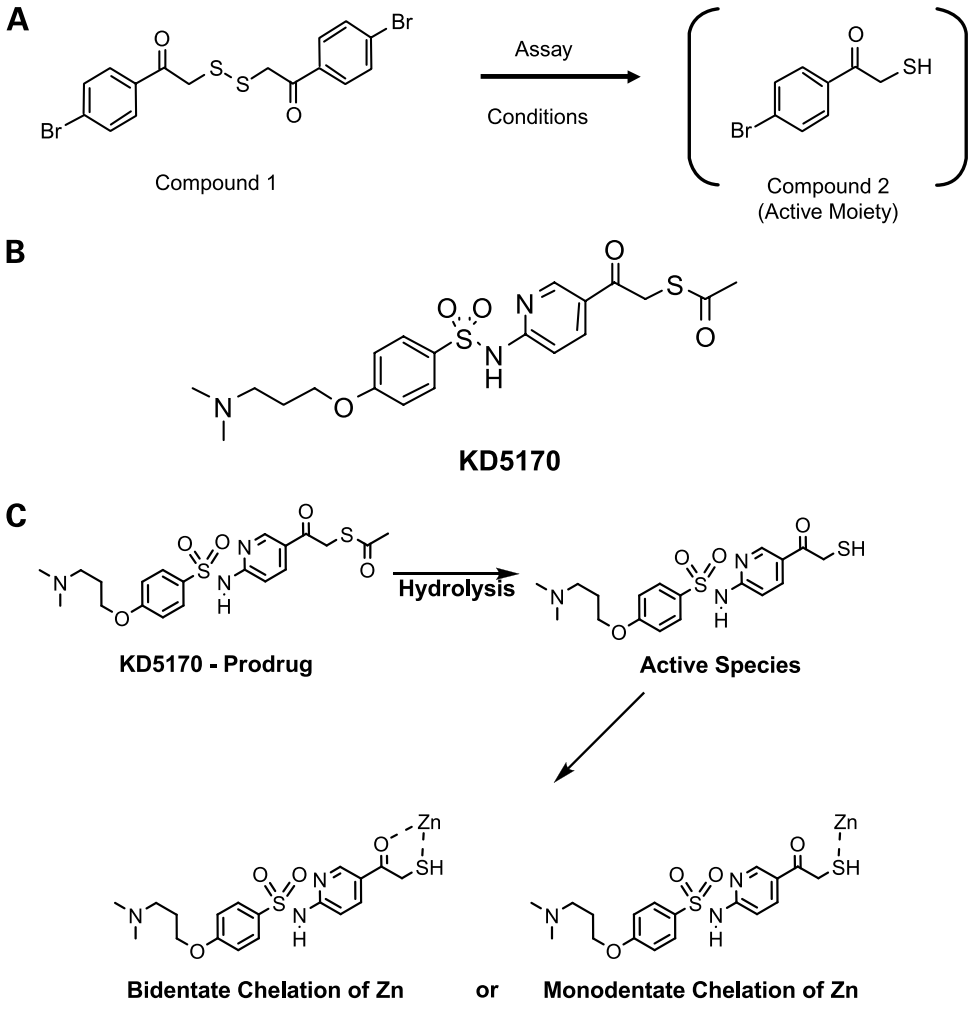

Figure 1. **A,** mercaptoketone series identified in a uHTS fluorescence-based biochemical screen. Compound 1 is readily reduced in the biochemical assay using HeLa cell nuclear extract generating two molar equivalents of active free thiol, compound 2. **B,** KD5170 is a mercaptoketone-based HDAC inhibitor delivered as a thioester-based prodrug. **C,** proposed mechanism of action. KD5170 thioester prodrug undergoes hydrolysis generating the mercaptoketone, which coordinates Zn^{2+} in a bidentate or monodentate fashion in the active site of HDACs.

Small molecule HDAC inhibitors have predominantly relied upon hydroxamic acid or, to a lesser extent, benzamide-based chemistry to enable high-affinity binding to HDACs (7). The inhibitory activity of hydroxamic acids stems from their ability to chelate zinc in the active site of both class I and class II enzymes, thereby arresting zinc-dependent enzymatic processes. Although hydroxamic acids can be potent inhibitors of HDACs and other Zn^{2+}-dependent metalloenzymes, they can also exhibit suboptimal pharmaceutical properties, such as low oral bioavailability and poor *in vivo* stability (9). By contrast, the one clinical stage natural product HDAC inhibitor, FK228, also inhibits HDACs by zinc binding but through a thiol group, a moiety well established as a metal chelator (9). The binding mode and mechanism of action of the benzamide class of HDAC inhibitors (CI-994, MS-275, and MGCD0103) is less clear, and unlike pan classes I and II inhibition by the hydroxamates, these compounds are relatively selective for class I isoforms (10). Cell-based assessment of the relative contribution of individual HDAC isoforms in tumor cell proliferation and apoptosis have largely implicated the class I enzymes HDAC1, HDAC2, and HDAC3, providing a rational basis for this selectivity profile (11, 12). However, the class II enzyme, HDAC6, has been identified recently as a modulator of the chaperone HSP90 (itself a therapeutic target for cancer; ref. 13) in addition to having a direct role in protein turnover as a component of the aggressome (14). Indeed, pharmacologic or genetic inhibition of HDAC6 combined with the proteasome inhibitor bortezomib results in synergistic lethality in various tumor cell lines (15–17). These data, coupled with the absence of an unequivocal link (e.g., mutation) between specific HDAC isoforms and development of human cancer, suggest that pan HDAC inhibitory activity may have the greatest clinical utility (7, 12, 18). With significant industry focus on hydroxamic acid–based and benzamide-based compounds, we sought to identify and develop novel nonhydroxamate, nonbenzamide broad spectrum HDAC inhibitors.

Materials and Methods

Cell Lines

Mantle cell lines Jeko-1, NCEB1, and Sp49 were obtained from Dr. Nori Kawamata of University of California-Los

Table 1. KD5170 inhibits both class I and class II HDAC isoforms

Compound	Recombinant human HDAC				
	HeLa	1	2	3	4
	$IC_{50} \pm$ SE (μmol/L)				
KD5170	0.045 ± 0.007	0.020 ± 0.004	2.06 ± 0.12	0.075 ± >0.01	0.026 ± 0.003
Compound 3 (disulfide)	0.014 ± 0.003	0.024 ± 0.007	0.74 ± 0.08	0.014 ± 0.003	0.023 ± 0.002
TSA	0.001 ± 0	0.012 ± 0.003	0.020 ± 0.0005	0.010 ± 0.005	0.022 ± 0.006

NOTE: HDAC activity was determined indirectly by measuring the fluorescence generated by a deacetylated fluorogenic peptide product (Materials and Methods). Data presented represent mean ± SE. KD5170 and compound 3, $n = 5$ replicate assay runs for HeLa cell nuclear extract and HDAC1, HDAC2, HDAC3, HDAC4, HDAC5, HDAC6, HDAC7, HDAC8, and HDAC10. HDAC9, $n = 3$. TSA, $n = 2$ for HeLa cell nuclear extract and all HDAC isoforms.

Angeles. Mantle cell lines SP53 and Z-138 were obtained from Dr. Jeff Medieros and Dr. Zeev Estrov of M. D. Anderson Cancer Center. Cutaneous T-cell lymphoma lines MJ, Hut78, and HH were obtained from American Type Culture Collection. NCI-60 human tumor cell lines were obtained through the National Cancer Institute, Division of Cancer Treatment.

High Throughput Screening

A biochemical assay was miniaturized to 1,536-well format for compatibility with the proprietary Kalypsys uHTS screening robot. Briefly, in each well, a single compound was incubated with partially purified HeLa cell nuclear extract (Accurate Scientific), followed by a 30-min incubation with a fluorogenic acetyl-lysine substrate, *Fluor de Lys* (BioMol). The reaction was stopped with developer reagent (BioMol), and fluorescent product was measured using an *Aquest* fluorometric plate reader (Molecular Devices). Data were processed using Kalypsys proprietary software and analyzed using Spotfire (Spotfire, Inc.). A minimal efficacy cutoff of 50% relative to trichostatin (1 μmol/L) identified hits for confirmation.

HeLa Cell Nuclear Extract and Recombinant Human HDAC Isoform Profiling

HDAC assays with HeLa cell nuclear extract were carried out at Kalypsys and Reaction Biology. IC_{50} values obtained were in close concordance with each other. Recombinant human HDAC isoform profiling was carried out by Reaction Biology. All enzymes were produced in SF9 insect cells as glutathione *S*-transferase fusion proteins and tested in reactions at the indicated concentrations to normalize for specific activity (Supplementary Methods).[3]

HDAC activity was determined indirectly by measuring the fluorescence generated by deacetylated fluorogenic peptide product reacting with a developer solution. All assays were carried out in the assay buffer (1×): 50 mmol/L Tris-HCl (pH 8.0), 137 mmol/L NaCl, 2.7 mmol/L KCl, 1 mmol/L $MgCl_2$, 1 mg/mL bovine serum albumin. Compound was added from a DMSO stock solution, and DMSO concentration was fixed across the dose range at 1%. Reactions were carried out at 30°C for 2 h and stopped with 0.5× Developer (RBC) + 2 μmol/L trichostatin A (TSA). Fluorogenic deacetylated product was detected using an Envision fluorimeter (Perkin-Elmer). Deacetylated standards were tested in replicate half-log dilutions starting at 50 μmol/L; background was determined in reactions using substrate in the absence of enzyme.

Cell-Based H3 and α-Tubulin Acetylation

HeLa cells (~5,000 per well) were allowed 8 to 24 h to adhere to wells of a 384-well Greiner polystyrene assay plate in media containing 10% serum. After cells have adhered, media were removed and cells were treated with compound in dose response for 18 hours. Cells were washed once with PBS (80 uL) and then fixed (40 μL of 95% ethanol, 5% acetic acid) for 1 min at room temperature. Cells were blocked with 2% bovine serum albumin for 1 h, washed, and then stained with rabbit anti–Ac-H3 antibody (Upstate Biotechnology; 1:2,000) or mouse anti–acetyl α-tubulin antibody (Sigma-Aldrich; 1:1,000), followed by washing and incubation with either a horseradish peroxidase–conjugated goat anti-rabbit IgG (Santa Cruz Biotechnology; 1:5,000) or goat anti-mouse IgG (Bio-Rad; 1:3,000). Signal was generated using Luminol substrate and detected using an Acquest multimode plate reader (Molecular Devices).

Mitochondrial Membrane Potential

HL-60 and HCT-116 cells were plated at 5×10^4 to 3×10^5 per well in a 96-well plate. KD5170 was added at designated concentrations (either by manual pipette or by Kalypsys proprietary passive pin-transfer) and incubated for 24 h (HL60) or 48 h (HCT-116). JC-1 dye (5,5′,6,6′-tetrachloro-1,1′,3,3′-tetraethylbenzimidazolylcarbocyanine iodide, Invitrogen) was added at 5 μg/well (diluted in media), thoroughly mixed, and incubated for 10 to 15 minutes at 37°C, 5% CO_2. Analysis was done with a BD LSRII fluorescent cell analyzer, using FL1 and FL2 variables.

Tumor Cell Cytotoxicity/NCI-60 Screen

Cells were grown and maintained in standard 15-cm diameter cell culture plates with RPMI 1640 containing 10% (v/v) fetal bovine serum and penicillin/streptomycin antibiotics (100 units/mL and 100 μg/mL final concentration, respectively). Cells were incubated with compounds in 1,536-well plates for 48 h before measurement of cellular

[3] Supplementary material for this article is available at Molecular Cancer Therapeutics Online (http://mct.aacrjournals.org/).

Table 1. KD5170 inhibits both class I and class II HDAC isoforms (Cont'd)

Recombinant human HDAC					
5	6	7	8	9	10
$IC_{50} \pm SE$ (μmol/L)					
0.95 ± 0.03	0.014 ± 0.002	0.085 ± 0.009	2.50 ± 0.34	0.15 ± 0.005	0.018 ± 0.001
0.36 ± 0.02	0.002 ± 0.0002	0.07 ± 0.009	0.58 ± 0.04	0.092 ± 0.008	0.015 ± 0.0009
0.016 ± 0.003	0.0020 ± 0	0.081 ± 0.04	0.12 ± 0.01	0.080 ± 0.04	0.028 ± 0.01

viability using ATPlite (Perkin-Elmer). This assay monitors the level of ATP in cells, a useful indicator of the cytotoxic, cytostatic, and antiproliferative effects of various agents (Supplementary Methods).[3]

Primary Patient Chronic Lymphocytic Leukemia Cytotoxicity

Peripheral blood draws from treatment-naive chronic lymphocytic leukemia patients were obtained from Scripps Cancer Center, Green Hospital (Dr. Allen Saven) as per institutional review board guidelines (IRB 04-602). Blood was centrifuged at 150 × *g* for 10 min at room temperature, and the serum was removed. Blood was diluted 1:2 with PBS (Ca^{2+} and Mg^{2+} free) and was layered on top of Ficoll-Paque Plus (Amersham). Samples were then centrifuged at 150 × *g* for 10 min at room temperature; the buffy coat layer was removed and centrifuged again. Isolated peripheral blood mononuclear cells were then resuspended in RPMI + 1% fetal bovine serum to 1.5×10^6 cells/mL. Cytotoxic activity of KD5170 was assessed using the Alamar Blue assay (Biosource). Cells (7,500) were plated per well in 384-well Greiner polystyrene assay plates, and compounds were added using Kalypsys proprietary passive pin transfer, followed by incubation for 24 to 48 h before analysis. Alamar Blue reagent (10% final concentration) was incubated for 6 h, and fluorescence was measured using an Acquest multimode plate reader (Molecular Devices).

Compound Formulation for *In vivo* Administration

All stated doses of KD5170 represent the dose of free-base. KD5170 (HBr salt) was formulated as a solution in sterile water (vehicle). Compound was placed in a 10-mL or 20-mL sterile dose vial, and an appropriate volume of water was added and mixed by vortexing to disperse. The formulation was heated to 40°C and vortexed until a clear solution was generated. Dose formulations were prepared just before use and used within 2 h. Docetaxel (Taxotere, Sanofi-Aventis) was supplied as a 40 mg/mL solution in Tween 80. On the day of dosing, an aliquot of docetaxel stock was mixed with an equal volume of 100% ethanol and then diluted with 5% dextrose in water to provide a 3 mg/mL solution (30 mg/kg dose). Likewise, to make a 1 mg/mL (10 mg/kg dose), docetaxel stock was mixed with two volumes of Tween 80 and three volumes of ethanol and then diluted with 5% dextrose in water. Final concentrations of vehicle for both docetaxel solutions were 7.5% ethanol, 7.5% Tween 80, and 85% of 5% dextrose in water.

In vivo Efficacy Studies

Female BALB/c *nu/nu* mice were purchased from Simonsen Laboratories, Inc. HCT-116 (5×10^6) and NCI-H460 (3×10^6) cells were injected s.c. in 100 μL of culture media. PC-3 tumors were passaged *in vivo* and injected as 1 mm^3 tumor fragments (PC-3 study was carried out at Piedmont Research Center). Tumors were monitored twice weekly and then daily as tumors approached 80 to 120 mm^3. Mice were then randomized based on tumor volume the day before start of treatment. Tumor size was monitored twice weekly by digital calipers, and body weight was recorded on the same days along with observations of general health. Tumor volume was calculated by the formula: $1 / 2 (x^2 y)$, wherein x = tumor width and y = tumor length. Time to end point (TTE) in the PC-3 study was calculated using the following formula: $TTE\ (d) = \log_{10}[\text{end point volume } (mm^3) - b / m]$, wherein b is the intercept and m is the slope of the line obtained by linear regression of a log-transformed tumor growth data set.

In vivo Pharmacodynamics

Female BALB/c *nu/nu* mice bearing HCT-116 xenograft tumors (group mean tumor volume, 277 mm^3; SD, ± 80 mm^3) received a single p.o. dose of KD5170 at 10, 30, or

Table 2. KD5170 is a potent inhibitor of HDAC activity cell-based assays

	Acetylation	
Compound	Histone H3, $EC_{50} \pm SE$ (μmol/L)	α-Tubulin, $EC_{50} \pm SE$ (μmol/L)
KD5170	0.025 μmol/L (±0.004; n = 20)	0.325 μmol/L (±0.1; n = 6)

NOTE: Cellular HDAC inhibitory activity in HeLa cells was assessed in a 384-well cytoblot using an antibody that recognizes acetylated histone H3 or acetylated α-tubulin. Cells were fixed and stained after a 7-h incubation with compound under standard HeLa cell culture conditions. Values shown represent a compilation of multiple independent experiments, as indicated (Materials and Methods).

100 mg/kg. At time points described, tumors were excised, snap frozen in liquid nitrogen, and stored at −80°C. Tumor lysates were made by mechanical disruption (Bio101 Fast Prep unit; speed, 5.0 for 30 s) with lysis buffer [50 mmol/L Tris (pH 8.0), 150 mmol/L NaCl, 0.02% sodium azide, 0.1% SDS, 1% NP40 substitute, 0.5% sodium deoxycholate, and complete protease inhibitor (Roche)]. Lysates were cleared by centrifugation and stored at −80°C until analyzed. Protein concentration was measured by the Bio-Rad detergent-compatible protein assay. One microliter of a 5 mg/mL total protein lysate was spotted onto nitrocellulose (Invitrogen) and allowed to dry for 15 min. The membrane was wetted in Tris-Gly gel blotting buffer (Invitrogen) plus 20% methanol for 5 min. The membrane was then rinsed with PBS for 2 min and blocked with Odyssey Blocking Buffer (LiCor) for 1 h at room temperature. Primary antibodies were incubated at the following concentrations: anti–Ac-H3 antibody 1:2,000 (Upstate Biotechnology), anti–α-tubulin 1:4,000 (Sigma-Aldrich), and anti–acetyl α-tubulin mouse monoclonal antibody (Sigma-Aldrich), all diluted in Odyssey Blocking Buffer at room temperature for 1 h. The membrane was then washed 4 × 5 min in TBS plus 0.1% Tween 20. Secondary antibodies were incubated at 1:10,000 dilution [goat anti-rabbit Alexa 680 (Invitrogen) and goat anti-mouse IR Dye 800 (Rockland)] in LiCor blocking buffer with 0.02% SDS and 0.1% Tween 20 for 1 h at room temperature. The membrane was washed 4 × 5 min in TBS plus 0.1% Tween 20 and 1 × 5 min in PBS and filter dried (dark). The membrane was scanned with the LiCor Odyssey Imaging System, and signal intensity was captured using manufacturer's protocol. Data were imported and analyzed in Microsoft Excel and plotted in Graph Pad Prism 5.0.

Western Blotting

Fifty micrograms of total protein were loaded and electrophophoresed on 4% to 20% Tris-glycine gels (Invitrogen). Proteins were transferred to nitrocellulose by electroblotting and subsequently processed in a similar manner to the arrays for LiCor analysis. Anti-human p21 mouse monoclonal antibody (Cell Signaling Technology) was diluted at 1:2,000 in Odyssey Blocking Buffer.

Identification of a Novel Series of HDAC Inhibitors

A 600,000 small molecule compound library was screened in a fluorescence-based biochemical assay that used the HDAC activity of a partially purified HeLa cell nuclear extract (19). This screen led to the identification of an α-mercaptoketone series of inhibitors. While compound 1 (Fig. 1A), a disulfide, was identified in the screen, the active species is the reduced, free thiol (compound 2) that is readily produced under our assay conditions (data not shown; note that the HeLa cell nuclear extract contains 12.5 μmol/L of the reducing agent DTT). This compound had an IC_{50} of 0.135 μmol/L, which was comparable with several hydroxamates also identified in the screen. Optimization of the α-mercaptoketone series has led to the clinical candidate KD5170 (Fig. 1B). The proposed mechanism of action is similar to that of the hydroxamic acids with the mercaptoketone moiety functioning as a bidentate or monodentate zinc binding group (Fig. 1C; ref. 9). The thiol functionality present in these molecules is intentionally protected as an inactive thioester due to the propensity of thiols to oxidatively dimerize in air and in solution. The thioester prodrug hydrolyzes relatively slowly under neutral and acidic conditions and more rapidly under basic conditions and undergoes facile enzymatic hydrolysis by esterases, such as those found in serum (data not shown). Nonhydrolyzable analogues of the series were inactive in biochemical and cell-based assays, indicating that the free thiol is the active species (data not shown).

Characterization of KD5170

In vitro Studies

KD5170 is a potent HDAC inhibitor *in vitro*, with an IC_{50} of 0.045 ± 0.007 μmol/L (SE; n = 5) in the HeLa cell nuclear extract screening assay (Table 1). To define the isoform selectivity of KD5170, biochemical assays with individual recombinant human enzymes were done (Table 1). TSA, the potent pan classes I and II inhibitor, was included as a positive control. Because the degree of KD5170 thioester hydrolysis and, therefore, the active thiol generated in these assays are not easily determined, a readily reduced disulfide of KD5170 (compound 3, analogous to compound 1 identified in the uHTS screen) was also profiled. The recombinant HDAC enzymes were synthesized as glutathione *S*-transferase fusions, and micromolar concentration of the reducing agent glutathione used to elute the proteins was still present in the reaction mixtures. Under these assay conditions, we predict that the disulfide was readily reduced, yielding two molar equivalents of active thiol. Among class I enzymes, KD5170 most potently inhibited HDAC1 [IC_{50}, 0.020 ± 0.004 μmol/L (SE); n = 5] and HDAC3 [IC_{50}, 0.075 ± 0.01 μmol/L (SE); n = 5]. KD5170 was a significantly less potent inhibitor of HDAC2 [IC_{50}, 2.0 ± 0.12 μmol/L (SE); n = 5], which is surprising because these two isoforms have the highest degree of amino acid homology (93%) among the class I enzymes (11). KD5170 also potently inhibited HDAC4 and HDAC6, with IC_{50} values of 0.026 μmol/L (SE, ±0.003 μmol/L; n = 5) and 0.014 μmol/L (SE, ±0.002 μmol/L; n = 5), respectively. After adjusting for two molar equivalents of the active thiol generated from each mole of disulfide, the IC_{50} values for KD5170 and compound 3 were roughly equivalent, suggesting that chemical conversion to the active free thiol species was comparable for both prodrugs.

In cell-based assays, KD5170 treatment resulted in concentration-dependent histone hyperacetylation with a low nanomolar potency [EC_{50}, 0.025 ± 0.004 μmol/L (SE); n = 20; Table 2; Supplementary Fig. S1].[3] The maximal response of KD5170 was similar to that of TSA, whose maximal effect was defined as the 100% response.

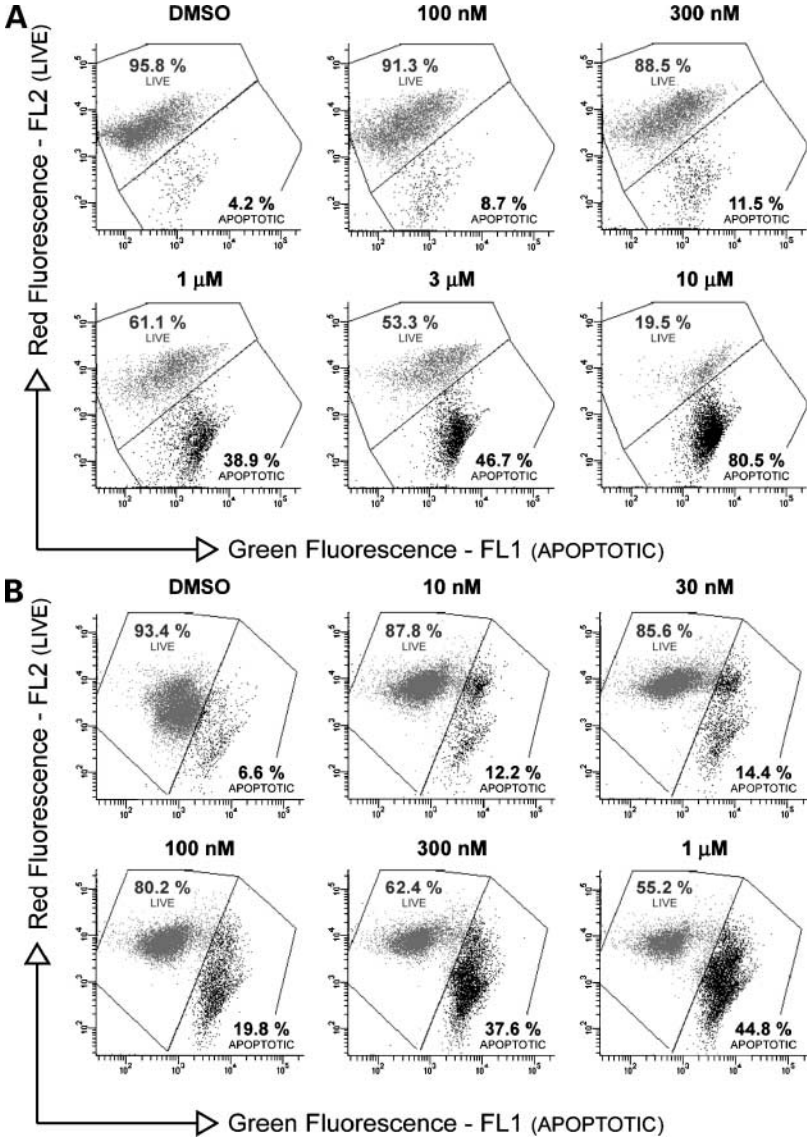

Figure 2. KD5170 induces apoptosis in human tumor cell lines. HCT-116 (**A**) human colorectal tumor cells and HL-60 (**B**) human leukemia cells were treated with KD5170 at increasing concentrations for a period of 48 and 24 h, respectively, followed by staining with JC-1 dye. Cytometric analysis was done using the BD LSRII fluorescent cell analyzer, and percentage of apoptotic versus healthy (live) cells are indicated (Materials and Methods).

Furthermore, KD5170 induced α-tubulin hyperacetylation, a surrogate for HDAC6 inhibition (20, 21), in HeLa cells [EC_{50} of 0.325 ± 0.1 μmol/L (SE), $n = 6$, or ~65% efficacy of TSA; Table 2]. Curiously, KD5170 potently and completely inhibited recombinant human HDAC6 activity with an IC_{50} of 0.014 μmol/L. The mechanistic basis of the partial inhibition of HDAC6, inferred from α-tubulin hyperacetylation in HeLa cells, is unclear.

Epigenetic transcriptional induction of the cell cycle inhibitor $p21^{WAF1}$ has been shown for many structurally diverse HDAC inhibitors and is thought to be a hallmark of HDAC inhibition (22–24). To determine if KD5170 induces p21 expression, HCT-116 cells were treated with increasing concentrations of KD5170 (30–1,000 nmol/L) for 6 and 18 h and p21 protein levels were monitored by quantitative Western blotting (Supplementary Fig. S2).[3] Similar to other HDAC inhibitors, KD5170 induced $p21^{WAF1}$ expression over the concentration range in which significant histone H3 and α-tubulin acetylation were also observed.

Multiple structurally distinct HDAC inhibitors have been reported to induce apoptosis of tumor-derived cells in culture (25). One central feature of apoptosis is disruption of mitochondrial membrane potential, which can be monitored by the fluorescent dye JC-1 (26). KD5170 induced cell death in a concentration-dependent manner in both HCT-116 colorectal cancer and HL-60 leukemia cells (Fig. 2A and B). In separate studies, a large subdiploid population of cells, indicative of nuclear DNA fragmentation, was observed after incubation with KD5170 and subsequent staining with propidium iodide and cytometric analysis (data not shown). KD5170 exhibits cytotoxic activities against the well-studied NCI-60 human tumor

cell line panel (ref. 23; Supplementary Table S1).[3] The cytotoxic activities (EC_{50}) ranged from 0.1 to 7.7 μmol/L, with a mean and median of 1.6 and 0.9 μmol/L, respectively. NCI-60 panel cell lines derived from hematologic cancers seemed to be more sensitive to KD5170, with EC_{50}s of ≤0.5 μmol/L against all six lines tested. We further profiled the cytotoxicity of KD5170 in primary cell isolates from treatment-naive chronic lymphocytic leukemia patients, as well as cell lines derived from cutaneous T-cell lymphoma and mantle cell lymphoma (Supplementary Table S1).[3] Submicromolar EC_{50}s were also observed, supporting the potential of KD5170 for treating hematologic malignancies.

KD5170 also exhibited significant cytotoxicity against a variety of cell lines derived from human solid tumors. Among the most sensitive cell lines was HCT-116 (EC_{50}, 0.14 μmol/L). Given the potent effect of KD5170, the utility of HCT-116 cells in the preclinical development of other HDAC inhibitors (24), and their favorable *in vivo* growth properties, we chose these cells to determine the pharmacodynamic response, antitumor activity, and dose optimization of KD5170 *in vivo*.

Tumor-Based Pharmacodynamics

HCT-116–bearing nude mice were given a single p.o. dose of KD5170 at 10, 30, or 100 mg (compound)/kg (body weight). Tumors were excised at 1, 2, 4, 8, and 24 h postdose (n = 4 per dose per time point). Whole-tumor lysates were monitored for histone H3 and α-tubulin acetylation by quantitative immunoblotting (Fig. 3A–C). An increase in histone H3 acetylation was observed as early as 1 h postdose (30 and 100 mg/kg), with further increases at 2 and 4 h. At 30 mg/kg, peak acetylation was detected at 4 h, whereas at 100 mg/kg, peak acetylation was achieved at 8 h. For all three doses, histone H3 acetylation was significantly decreased from peak by 24 h; however, it was still modestly above the baseline. This pharmacodynamic response is consistent with the pharmacokinetics

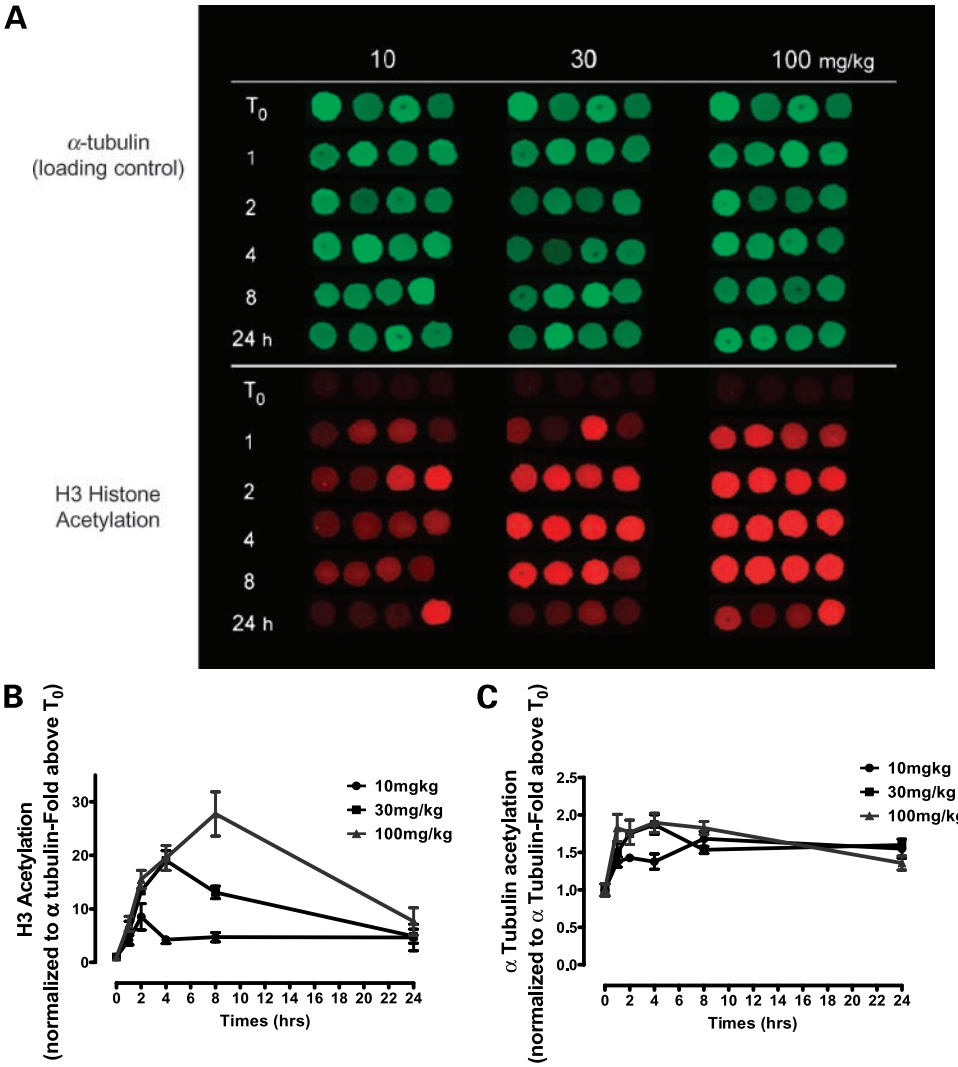

Figure 3. KD5170 induces a robust and sustained pharmacodynamic response in xenograft tumor tissues. HCT-116 tumor-bearing mice were p.o. given a single dose of KD5170 at 10, 30, or 100 mg/kg. Tumor tissue was excised and snap frozen at times indicated, and histone H3 (**A** and **B**) and α-tubulin acetylation (**C**) was quantified by immunoblotting and LiCor imaging technology. Total α-tubulin was used to normalize for amount of protein spotted. Points, mean; bars, SE (n = 4 tumors per time point per dose group). The T_0 data points used for normalization were the same for each treatment and graphically replicated in Fig. 3A for ease of comparison.

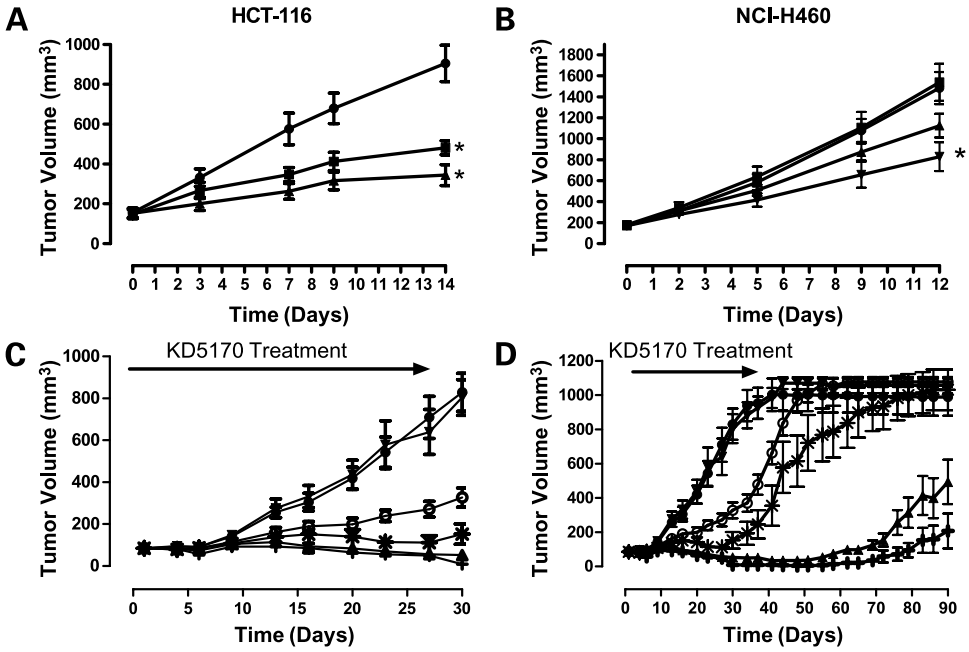

Figure 4. KD5170 inhibits growth of HCT-116, NCI-H460, and PC-3 cell lines *in vivo*. **A,** HCT-116. KD5170 p.o. inhibits tumor growth in a human colon cancer (HCT-116) xenograft. Vehicle, ●; KD5170 (42 mg/kg), ■; KD5170 (84 mg/kg), ▲. Points, mean; bars, SE (n = 7 mice per dose group). **B,** NCI-H460. Vehicle, ■; erlotinib (100 mg/kg), ●; KD5170 (32 mg/kg), ▲; KD5170 (64 mg/kg), ▼. Points, mean; bars, SE (n = 8 mice per dose group). T/C, (treated final volume − treated initial volume) / (control final volume − control initial volume) × 100. A T/C value of 0 equals tumor stasis. *, $P < 0.05$. Statistical significance was determined by t test: two-sample assuming unequal variances (control versus treated on last measurement point). **C,** PC-3 end of treatment, day 30. No treatment, ●; vehicle, ▼; KD5170 (30 mg/kg qod), ○; docetaxel (10 mg/kg i.v.), *; docetaxel (30 mg/kg i.v.), +; KD5170 (30 mg/kg qod) and docetaxel (10 mg/kg i.v.), ▲. Points, mean; bars, SE (n = 10 mice per dose group). **D,** PC-3 tumor regrowth posttreatment, day 90. No treatment, ●; vehicle, ▼; KD5170 (30 mg/kg qod), ○; docetaxel (10 mg/kg i.v.), *; docetaxel (30 mg/kg i.v.), +; KD5170 (30 mg/kg qod) and docetaxel (10 mg/kg i.v.), ▲. Points, mean; bars, SE (n = 10 mice per dose group).

of KD5170 after p.o. dosing in mice (data not shown). α-tubulin acetylation was also observed, although the magnitude of induction over baseline was significantly lower than that detected for histone H3. Peak α-tubulin acetylation was observed at 4 h post–single dose at both 30 and 100 mg/kg, with levels returning to near baseline by 24 h.

Table 3. KD5170 dose optimization in HCT-116 xenograft tumor bearing mice

Dose (mg/kg)	Regimen	T/C	Bodyweight	Mortality
8.4	qd × 7	107%	−2%	0/5
25	qd × 7	59%	−9.6%	0/5
42	qd × 7	11%	−22%	6/10
42	qd × 5	24%	−12%	3/8
42	**qod × 7**	**44%**	**−2%**	**0/7**
84	**qod × 7**	**17%**	**−8.7%**	**1/7**
25	qod × 10	55%	−1.5%	0/8
50	qod × 10	35%	−2.4%	0/8
50	qod × 11	63%	−2.6%	0/10
75	qod × 11	35%	−12.9%	3/10
100	qod × 11	35%	−15.7%	8/10

NOTE: Compilation of a series of HCT-116 xenograft experiments comparing efficacy and tolerability of different dose regimens of KD5170. T/C, (treated final volume − treated initial volume) / (control final volume − control initial volume) × 100. Bodyweight at day after last dose relative to that at start. Mortality, number of animals that died or were sacrificed due to overt toxicity.

In vivo Efficacy: Monotherapy

Based on outcomes from a series of dose optimization studies using HCT-116 tumor–bearing nude mice, an every other day (qod) p.o. dosing regimen was selected (Fig. 4A and Table 3). This regimen increased the therapeutic index of KD5170 by reducing toxicity and maintaining significant efficacy. At 42 and 84 mg/kg qod, significant tumor growth inhibition was observed with treated versus control (T/C) values of 44% and 25%, respectively. KD5170 was well tolerated at 42 mg/kg qod with no apparent toxicity based on body weight changes (Table 3, *bold font*). The 84 mg/kg qod dose was associated with a mean body weight loss of 8.7%, and one death of seven animals, indicating a maximum tolerated dose between 42 and 84 mg/kg qod in this setting. In independent experiments to assess effects on hematopoietic system (complete blood counts) in wild-type BALB/c mice, KD5170 at 50 and 100 mg/kg qd and qod × 7 resulted in a pan-cytopenia indicative of myeloid suppression (data not shown). Histopathologic assessment of both spleen and sternum (bone marrow) in these animals indicated that both the lymphoid and myeloid compartments were

Table 4. KD5170 inhibits tumor growth in a human prostate cancer PC-3 xenograft

Compound 1	Compound 2	T/C	Bodyweight nadir (d)
No treatment			0
Vehicle 1	Vehicle 2		0
KD5170 30 mg/kg qod × 14		32%	0
	Docetaxel 10 mg/kg qwk × 3	9%	0
	Docetaxel 30 mg/kg qwk × 3	−4%	−5.7% (d23)
KD5170 30 mg/kg qod × 14	Docetaxel 10 mg/kg qwk × 3	−11%	6.5% (d20)

NOTE: T/C values at day 30 measurement point. Bodyweight nadir and day on which it was observed. A T/C value of 0 equals tumor stasis.

targeted. These data are consistent with published reports of myeloid suppression in both preclinical and clinical studies of structurally diverse HDAC inhibitors and is consistent with HDAC inhibition.

Antitumor growth effects were also observed in xenografts of NCI-H460 cells, a rapidly growing non–small cell lung carcinoma line that is insensitive to a variety of therapeutics *in vitro* and *in vivo*, including the epidermal growth factor receptor inhibitor erlotinib (Tarceva; refs. 27, 28). KD5170 was cytotoxic to NCI-H460 cells *in vitro* with an EC_{50} of 0.23 μmol/L (Supplementary Table S1).[3] Consistent with published findings, erlotinib did not inhibit growth of NCI-H460 tumors at p.o. doses as high as 100 mg/kg qd, a dose previously shown to cause tumor stasis in xenograft tumors of other cell lines (ref. 29; Fig. 4B). By contrast, KD5170 inhibited the growth of NCI-H460, with a significant effect observed at 60 mg/kg qod (T/C 48%). Cumulatively, these data indicate that KD5170 significantly inhibited the growth of xenograft tumors derived from two distinct tumor types.

In vivo Efficacy: Combination Therapy

Preclinical data supports the use of HDAC inhibitors in prostate cancer (28). HDAC inhibition can result in reduced expression of the androgen receptor in androgen-dependent prostate cancer cell lines, resulting in impaired cell proliferation and/or increased apoptosis (30). In addition, the HDAC inhibitors vorinostat and LBH589 have been shown to inhibit the growth of the androgen receptor–independent prostate cancer cell line PC-3 *in vivo* (31, 32). To determine the potential for KD5170 in treating prostate cancer, we treated PC-3 xenograft–bearing nude mice with KD5170 alone or in combination with the standard of care agent docetaxel. Optimal combination doses of these two agents were first determined in a maximum tolerated dose study in non–tumor-bearing female nude mice (data not shown). Based on this study, KD5170 was dosed at 30 mg/kg qod × 14 as monotherapy and in combination with 10 mg/kg docetaxel dosed once weekly (qwk) × 3 (1/3 maximum tolerated dose). In addition, a separate arm of docetaxel at 30 mg/kg qwk × 3 (maximum tolerated dose) was included as a reference (maximum efficacy). KD5170 at 30 mg/kg qod inhibited the growth of PC-3 xenograft tumors with a day 30 (end of treatment period) T/C value of 32% (Fig. 4C; Table 4). This dose of KD5170 was well tolerated with no body weight loss (Table 4). Both doses of docetaxel alone significantly inhibited tumor growth with T/C values of 9% and 4%, respectively. It is of note that the KD5170/docetaxel combination caused tumor stasis or even modest regression at day 30 with a T/C value of −11%. Whereas there was no significant difference in effect between the KD5170/docetaxel combination and docetaxel alone (10 mg/kg qwk × 3) at day 30, a different picture emerged when tumor growth was monitored for 60 days post–treatment period (Fig. 4D). Median TTE (1,000 mm^3) was significantly increased (log-rank test) in the KD5170 and docetaxel monotherapy arms (Table 5). Interestingly, TTE in the KD5170/docetaxel combination arm was not only

Table 5. KD5170 and docetaxel combination results in a significant delay in TTE

Compound 1	Compound 2	MTV (mm^3), (in study; day 90)	Fraction at endpoint (1,000 mm^3)	TTE
No treatment		40	9/10	33
Vehicle 1	Vehicle 2	—	10/10	31
KD5170 30 mg/kg qod × 14		—	10/10	47*
	Docetaxel 10 mg/kg qwk × 3	40	9/10	60*
	Docetaxel 30 mg/kg qwk × 3	206	0/5	90*
KD5170 30 mg/kg qod × 14	Docetaxel 10 mg/kg qwk × 3	479	1/9	90*†

NOTE: Tumor growth was monitored twice weekly for 60 d post last dose of KD5170. Fraction at end point represents the fraction of mice that reached end point (1,000 mm^3) by day 90. TTE represents the median time for a tumor to reach the end point in days (Materials and Methods).

* Denotes significant log-rank test versus vehicle and no treatment controls ($P = 0.0040$).

† Denotes significant log-rank test versus corresponding monotherapy arms [docetaxel 10 mg/kg qwk ($P = 0.0056$) × 3 or KD5170 30 mg/kg QOD × 14 ($P = 0.0002$)].

Table 6. KD5170 and docetaxel combination results in an increase in number of tumor regressions

Compound 1	Compound 2	Regressions		
		PR	CR	TFS
No treatment		0	0	0
Vehicle 1	Vehicle 2	0	0	0
KD5170 30 mg/kg qod × 14		0	0	0
	Docetaxel 10 mg/kg qwk × 3	1	1	1
	Docetaxel 30 mg/kg qwk × 3	2	3	0
KD5170 30 mg/kg qod × 14	Docetaxel 10 mg/kg qwk × 3	4	1	0

NOTE: Partial regression is when the tumor volume was 50% or less than that of day 1 for three consecutive measurements during the course of study and $\geq$13.5 mm^3 for one or more of these three measurements. Complete regression is when the tumor volume was <13.5 mm^3 for three consecutive measurements during course of study. An animal with a complete remission at termination of study is classified as a tumor-free survivor.
Abbreviations: PR, partial regression; CR, complete regression; TFS, tumor-free survivor.

significant compared with no treatment and vehicle controls but also with docetaxel 10 mg/kg qwk × 3 with only one of nine tumors reaching 1,000 mm^3 by study end, and hence, a median TTE of >90 days. In addition, there was an increase in number of tumor regressions in the KD5170/docetaxel combination arm over that observed in either of the corresponding monotherapy arms (Table 6).

Discussion

Epigenetic subversion of key regulatory pathways is a hallmark of human cancer (33). Integral to this process is the posttranslational modification of histones, finely regulated by the opposing activities of histone acetyltransferases and HDACs (2). Highly acetylated histones are associated with a chromatin state that facilitates active transcription. However, treatment of cells with HDAC inhibitors results not only in transcriptional up-regulation, but also transcriptional down-regulation, resulting in altered expression of 2% to 20% of all genes (34–36). More recently, it has become clear that HDACs also have many nonhistone substrates, including key modulators of oncogenesis, such as p53, HSP90, STAT, Bax, nuclear factor-κB, etc. (5). Together, acetylation (and therefore inhibition) of histone and nonhistone substrates by HDACs results in the modulation of a multitude of signaling cascades and cellular processes that are just beginning to be defined.

Like hydroxamic acids, thiols have long been appreciated as potent zinc chelators. This moiety has been used in different compounds to inhibit a diverse array of zinc-dependent enzymes, including angiotensin-coverting enzyme (2, 34, 37), matrix metalloproteinases (38), and, more recently, HDACs (9). With respect to HDACs, the bacterial natural product FK228 (romidepsin) was the first thiol-based HDAC inhibitor to enter clinical development (39). FK228 is currently in phase II/phase III clinical trials and is exhibiting a therapeutic signal in several cancer types, including peripheral and cutaneous T-cell lymphoma and prostate cancer. Taking a cue from FK228, rationally designed thiol-based small molecule HDAC inhibitors have been described (8, 9). Broadly, these small molecule agents use the potent zinc coordinating activity of sulfur, with potential for p.o. administration and ease of synthesis not possible with macrocyclic compounds, such as FK228. Emblematic of this approach are a series of thiol-based vorinostat analogues, which are reported to be as potent as their parent hydroxamate in biochemical assays (9, 40). Additional efforts have focused on generating mercaptoacetoamide-based compounds that are thought to chelate the HDAC–active site zinc in either a monodentate or bidentate fashion, similar to that proposed for KD5170 (41). Our preliminary analysis suggests that both mercaptoacetoamides and alkylmercaptans are less potent than the corresponding mercaptoketones.[4] Many of the mercaptoacetoamides have been identified in the academic sector with little published data on *in vivo* pharmacokinetics, pharmacodynamics, antitumor efficacy, or other variables of pharmaceutical potential. It remains to be seen if any of these agents progress to clinical development.

KD5170, a unique mercaptoketone, is the end product of a chemical screen and subsequent medicinal chemistry effort to maximize broad spectrum potency and optimize physicochemical properties, such as aqueous solubility. KD5170 has a unique HDAC isoform selectivity profile in that it is a more potent inhibitor of HDAC1/HDAC3 than HDAC2 and also potently inhibits class II enzymes (e.g., HDAC6). This is distinct from the pan inhibitory activity of the clinical hydroxamates, in addition to that of the benzamides, which exhibit selectivity for a subset of class I enzymes (10). It is likely that different tumor types use a different subset of HDACs to their selective advantage, and hence, an *a priori* prediction is that agents with a broader inhibitory profile will have clinical utility across a wider range of human cancers (42). Insight into the optimal inhibitory profile should have been gleaned from the clinical evaluation of HDAC inhibitors with diverse selectivity profiles across various cancer indications.

KD5170 is cytotoxic to a broad range of human tumor-derived cell lines. This cytotoxicity results from induction of apoptosis, as monitored by alteration in mitochondrial

[4] Hassig CA, Smith ND, and Hager JH, unpublished observation.

membrane potential and DNA fragmentation in both the HCT-116 and HL-60 cell lines. The ability to induce tumor cell death via apoptosis is consistent with the proapoptotic activity observed for other HDAC inhibitors (43). With the KD5170 NCI-60 cytotoxicity profile and the wealth of publicly accessible pharmacogenomic data for this tumor cell panel, correlations between therapeutic response and tumor type, mutational status and sensitivity to other agents can be established (23, 44–46). These data will provide the groundwork for future screens to identify novel therapeutic combinations and guide selection of clinical indications.

A single p.o. dose of KD5170 induces dose-dependent histone H3 acetylation in HCT-116 xenograft tumors. Induction is first observed at 1 hour, the earliest time point monitored, and exhibits a significant trend toward baseline by 24 hours, an effect consistent with its pharmacokinetic profile. Whereas there is a modest induction of histone H3 acetylation at 10 mg/kg, this dose is not sufficient to mediate an antitumor response when dosed once daily in HCT-116 xenografts (Table 3). In the dose range that yields significant antitumor response (30–100 mg/kg), significant histone H3 acetylation was observed above baseline for $\geq$8 hours post–single dose, indicating that this represents the magnitude and duration of response necessary to mediate an antitumor effect. This pharmacodynamic response and its relationship to pharmacokinetics will help guide optimal dose selection in man. KD5170 also exhibits significant single-agent activity in xenografts of NCI-H460 (non–small cell lung carcinoma) and PC-3 (prostate) cell lines, along with increased antitumor effects in combination with docetaxel in the PC-3 model. The activity in combination with docetaxel supports the hypothesis that HDAC inhibitors will ultimately be most efficacious when used in combination therapy, as are many ''molecularly targeted'' cancer therapeutics (47). Future studies will continue to explore this combination with a focus on optimization of dose order and regimen. In addition to the activity in solid tumor xenografts, KD5170 has recently been shown to exhibit significant activity against multiple myeloma cell lines *in vitro* and *in vivo*.[5] The *in vitro* and *in vivo* profiles of KD5170, coupled with its pharmaceutical attributes, support continued preclinical and clinical development as a p.o. given therapeutic with potential across a wide range of cancer indications.

Disclosure of Potential Conflicts of Interest

A. Saven: Kalypsis, Inc., scientific advisory board; J.H. Hager: former Kalypsis, Inc., employee and current stockholder. The other authors disclosed no potential conflicts of interest.

Acknowledgments

We thank Dr. Nori Kawamata (University of California-Los Angeles) for the mantle cell lines Jeko-1, NCEB1, and Sp49; Dr. Jeff Medeiros and Dr. Zeev Estrov for the mantle cell lines Jeko-1, SP53, and Z-138 (M. D. Anderson Cancer Center); John McNeil and Brian Bolt (Kalypsys) for statistical analysis of NCI-60 data; and Chassidy Hall and the team at Piedmont Research Center for the PC-3 xenograft study.

[5] R. Feng, H. Ma, C.A. Hassig, et al. KD5170, a novel mercaptoketone-based HDAC inhibitor, exerts potent anti-myeloma effects by DNA damage and mitochondrial signaling. Molecular Cancer Therapeutics. In press, 2008.

References

1. Minucci S, Pelicci PG. Histone deacetylase inhibitors and the promise of epigenetic (and more) treatments for cancer. Nat Rev Cancer 2006;6:38–51.

2. Wang GG, Allis CD, Chi P. Chromatin remodeling and cancer. Part I. Covalent histone modifications. Trends Mol Med 2007;13:363–72.

3. Gallinari P, Di MS, Jones P, Pallaoro M, Steinkuhler C. HDACs, histone deacetylation and gene transcription: from molecular biology to cancer therapeutics. Cell Res 2007;17:195–211.

4. Xu WS, Parmigiani RB, Marks PA. Histone deacetylase inhibitors: molecular mechanisms of action. Oncogene 2007;26:5541–52.

5. Glozak MA, Sengupta N, Zhang X, Seto E. Acetylation and deacetylation of non-histone proteins. Gene 2005;363:15–23.

6. Kouzarides T. Acetylation: a regulatory modification to rival phosphorylation? EMBO J 2000;19:1176–9.

7. Glaser KB. HDAC inhibitors: clinical update and mechanism-based potential. Biochem Pharmacol 2007;74:659–71.

8. Marks PA. Discovery and development of SAHA as an anticancer agent. Oncogene 2007;26:1351–6.

9. Suzuki T, Miyata N. Non-hydroxamate histone deacetylase inhibitors. Curr Med Chem 2005;12:2867–80.

10. Khan N, Jeffers M, Kumar S, et al. Determination of the class and isoform selectivity of small molecule HDAC inhibitors. Biochem J 2008;409:581–9.

11. de Ruijter AJ, van Gennip AH, Caron HN, Kemp S, van Kuilenburg AB. Histone deacetylases (HDACs): characterization of the classical HDAC family. Biochem J 2003;370:737–49.

12. Glaser KB, Li J, Staver MJ, Wei RQ, Albert DH, Davidsen SK. Role of class I and class II histone deacetylases in carcinoma cells using siRNA. Biochem Biophys Res Commun 2003;310:529–36.

13. Bali P, Pranpat M, Bradner J, et al. Inhibition of histone deacetylase 6 acetylates and disrupts the chaperone function of heat shock protein 90: a novel basis for antileukemia activity of histone deacetylase inhibitors. J Biol Chem 2005;280:26729–34.

14. Kawaguchi Y, Kovacs JJ, McLaurin A, Vance JM, Ito A, Yao TP. The deacetylase HDAC6 regulates aggresome formation and cell viability in response to misfolded protein stress. Cell 2003;115:727–38.

15. Catley L, Weisberg E, Kiziltepe T, et al. Aggresome induction by proteasome inhibitor bortezomib and α-tubulin hyperacetylation by tubulin deacetylase (TDAC) inhibitor LBH589 are synergistic in myeloma cells. Blood 2006;108:3441–9.

16. Hideshima T, Bradner JE, Wong J, et al. Small-molecule inhibition of proteasome and aggresome function induces synergistic antitumor activity in multiple myeloma. Proc Natl Acad Sci U S A 2005;102:8567–72.

17. Nawrocki ST, Carew JS, Pino MS, et al. Aggresome disruption: a novel strategy to enhance bortezomib-induced apoptosis in pancreatic cancer cells. Cancer Res 2006;66:3773–81.

18. Karagiannis TC, El-Osta A. Will broad-spectrum histone deacetylase inhibitors be superseded by more specific compounds? Leukemia 2007;21:61–5.

19. Hassig CA, Tong JK, Fleischer TC, et al. A role for histone deacetylase activity in HDAC1-mediated transcriptional repression. Proc Natl Acad Sci U S A 1998;95:3519–24.

20. Matsuyama A, Shimazu T, Sumida Y, et al. *In vivo* destabilization of dynamic microtubules by HDAC6-mediated deacetylation. EMBO J 2002;21:6820–31.

21. Hubbert C, Guardiola A, Shao R, et al. HDAC6 is a microtubule-associated deacetylase. Nature 2002;417:455–8.

22. Sowa Y, Orita T, Minamikawa S, et al. Histone deacetylase inhibitor activates the WAF1/Cip1 gene promoter through the Sp1 sites. Biochem Biophys Res Commun 1997;241:142–50.

23. Shoemaker RH. The NCI60 human tumour cell line anticancer drug screen. Nat Rev Cancer 2006;6:813–23.

24. Remiszewski SW. The discovery of NVP-LAQ824: from concept to clinic. Curr Med Chem 2003;10:2393–402.

25. Marks PA, Richon VM, Rifkind RA. Histone deacetylase inhibitors: inducers of differentiation or apoptosis of transformed cells. J Natl Cancer Inst 2000;92:1210 – 6.

26. Salvioli S, Ardizzoni A, Franceschi C, Cossarizza A. JC-1, but not DiOC6(3) or rhodamine 123, is a reliable fluorescent probe to assess $\delta\psi$ changes in intact cells: implications for studies on mitochondrial functionality during apoptosis. FEBS Lett 1997;411:77 – 82.

27. Thomson S, Buck E, Petti F, et al. Epithelial to mesenchymal transition is a determinant of sensitivity of non-small-cell lung carcinoma cell lines and xenografts to epidermal growth factor receptor inhibition. Cancer Res 2005;65:9455 – 62.

28. Zhang Z, Karam J, Frenkel E, Sagalowsky A, Hsieh JT. The application of epigenetic modifiers on the treatment of prostate and bladder cancer. Urol Oncol 2006;24:152 – 60.

29. Pollack VA, Savage DM, Baker DA, et al. Inhibition of epidermal growth factor receptor-associated tyrosine phosphorylation in human carcinomas with CP-358,774: dynamics of receptor inhibition *in situ* and antitumor effects in athymic mice. J Pharmacol Exp Ther 1999; 291:739 – 48.

30. Chen L, Meng S, Wang H, et al. Chemical ablation of androgen receptor in prostate cancer cells by the histone deacetylase inhibitor LAQ824. Mol Cancer Ther 2005;4:1311 – 9.

31. Butler LM, Agus DB, Scher HI, et al. Suberoylanilide hydroxamic acid, an inhibitor of histone deacetylase, suppresses the growth of prostate cancer cells *in vitro* and *in vivo*. Cancer Res 2000;60:5165 – 70.

32. Qian DZ, Kato Y, Shabbeer S, et al. Targeting tumor angiogenesis with histone deacetylase inhibitors: the hydroxamic acid derivative LBH589. Clin Cancer Res 2006;12:634 – 42.

33. Baylin SB, Chen WY. Aberrant gene silencing in tumor progression: implications for control of cancer. Cold Spring Harb Symp Quant Biol 2005;70:427 – 33.

34. Glaser KB, Staver MJ, Waring JF, Stender J, Ulrich RG, Davidsen SK. Gene expression profiling of multiple histone deacetylase (HDAC) inhibitors: defining a common gene set produced by HDAC inhibition in T24 and MDA carcinoma cell lines. Mol Cancer Ther 2003;2:151 – 63.

35. Mitsiades CS, Mitsiades NS, McMullan CJ, et al. Transcriptional signature of histone deacetylase inhibition in multiple myeloma: biological and clinical implications. Proc Natl Acad Sci U S A 2004; 101:540 – 5.

36. Peart MJ, Smyth GK, van Laar RK, et al. Identification and functional significance of genes regulated by structurally different histone deacetylase inhibitors. Proc Natl Acad Sci U S A 2005;102:3697 – 702.

37. Rubin B, Antonaccio MJ, Horovitz ZP. Captopril (SQ 14,225) (D-3-mercapto-2-methylpropranoyl-L-proline): a novel orally active inhibitor of angiotensin-converting enzyme and antihypertensive agent. Prog Cardiovasc Dis 1978;21:183 – 94.

38. Naglich JG, Jure-Kunkel M, Gupta E, et al. Inhibition of angiogenesis and metastasis in two murine models by the matrix metalloproteinase inhibitor, BMS-275291. Cancer Res 2001;61:8480 – 5.

39. Marshall JL, Rizvi N, Kauh J, et al. A phase I trial of depsipeptide (FR901228) in patients with advanced cancer. J Exp Ther Oncol 2002;2: 325 – 32.

40. Suzuki T, Kouketsu A, Matsuura A, et al. Thiol-based SAHA analogues as potent histone deacetylase inhibitors. Bioorg Med Chem Lett 2004;14:3313 – 7.

41. Vanommeslaeghe K, Loverix S, Geerlings P, Tourwe D. DFT-based ranking of zinc-binding groups in histone deacetylase inhibitors. Bioorg Med Chem 2005;13:6070 – 82.

42. Nakagawa M, Oda Y, Eguchi T, et al. Expression profile of class I histone deacetylases in human cancer tissues. Oncol Rep 2007;18:769 – 74.

43. Marks PA, Jiang X. Histone deacetylase inhibitors in programmed cell death and cancer therapy. Cell Cycle 2005;4:549 – 51.

44. Blower PE, Verducci JS, Lin S, et al. MicroRNA expression profiles for the NCI-60 cancer cell panel. Mol Cancer Ther 2007;6:1483 – 91.

45. Ikediobi ON, Davies H, Bignell G, et al. Mutation analysis of 24 known cancer genes in the NCI-60 cell line set. Mol Cancer Ther 2006;5:2606 – 12.

46. Bussey KJ, Chin K, Lababidi S, et al. Integrating data on DNA copy number with gene expression levels and drug sensitivities in the NCI-60 cell line panel. Mol Cancer Ther 2006;5:853 – 67.

47. Karagiannis TC, El-Osta A. Clinical potential of histone deacetylase inhibitors as stand alone therapeutics and in combination with other chemotherapeutics or radiotherapy for cancer. Epigenetics 2006;1:121 – 6.